Polyoxometalates

DOI: 10.1002/ange.201107481

Hybrid Assemblies of Eu-Containing Polyoxometalates and Hydrophilic Block Copolymers with Enhanced Emission in Aqueous Solution**

Jie Zhang, Yang Liu, Yang Li, Hongxiang Zhao, and Xinhua Wan**

Polyoxometalates (POMs), a type of giant transition metal oxide clusters on the nanoscale, are emerging as useful materials with unique catalytic, electrooptical, and biological properties.[1,2] Lanthanide-containing POMs elements show excellent photoluminescent properties with narrow emission bands, large Stokes shift, long lifetime, and tunable emission, i.e., their long emission timescale (micro- to milliseconds) also allows autofluorescence from the biological samples to be removed by time-gating the emission decay.[3] Therefore they are attractive for labeling and imaging of biological molecules.

In spite of their intriguing functionality, practical POM-based materials are quite scarce because of their inherent limitations, that is, poor processability in the solid state and weakened functionality in solution. For example, the Eu-containing POM $Na_9EuW_{10}O_{36}\cdot 32H_2O$ displays only weak photoluminescence in water in comparison to the solid state due to fluorescence quenching by water molecules.[3] Therefore, the development of supramolecular methodologies to protect and utilize POMs is important for application of POMs. Polymers are ideal protective matrices for this purpose, into which POMs were incorporated to fabricate supramolecular assemblies for improved processability and enhanced functionality. Besides the widely used layer-by-layer assembly of POMs with polyelectrolytes for functional thin films, polymerizable surfactants and amphiphilic block copolymers have been used to organize POMs into stable supramolecular assemblies in organic solution.[4–6] As far as we know, there are still no reports on the emission enhancement of lanthanide-containing POMs in aqueous solutions through supramolecular assembly strategies.

Herein we report a straightforward procedure to fabricate hybrid assemblies of lanthanide-containing POMs with block copolymers in aqueous solution. Core–shell nanostructured organic–inorganic hybrid materials were produced by direct mixing of $Na_9EuW_{10}O_{36}\cdot 32H_2O$ (Eu-POM) with double-hydrophilic neutral–cationic block copolymer poly(ethylene oxide-*b*-*N*,*N*-dimethylaminoethyl methacrylate) (PEO-*b*-PDMAEMA) in aqueous solution (Scheme 1). Neither

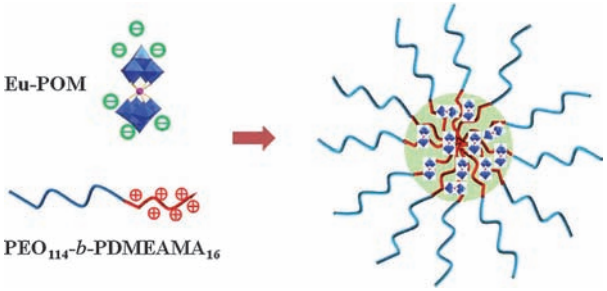

Scheme 1. Representative structures of double-hydrophilic neutral–cationic block copolymer PEO_{114}-*b*-$PDMEAMA_{16}$ and anionic polyoxometalate $Na_9EuW_{10}O_{36}\cdot 32H_2O$ and core–shell nanostructures of their complex in water.

PEO-*b*-PDMAEMA (pH 6.0 at a concentration of 4.42 mg mL^{-1}) nor Eu-POM is capable of self-assembling into nanostructures before mixing. On mixing, core–shell micellization is driven by the electrostatic interaction between the cationic PDMAEMA segment and the anionic Eu-POM. The micellar core is composed of the electrostatic hybrid complex, stabilized by the neutral PEO segments as the shell. These kinds of core–shell micelles have been coined "complex coacervate core micelles" (C3Ms).[7] The C3Ms are suitable carrier and reactor systems in bioinspired fields such as drug and gene delivery, controlled release, and biosensors, due to their high structural stability, chemical diversity, stimulus sensitivity, and site-recognition properties.[8–10]

In the present work, the hybrid C3M was prepared by titration of the block copolymer into a solution of Eu-POM. Formation of nano-assemblies of the hybrid complex was tracked by light scattering. The initial scattered intensity of the Eu-POM solution at a scattering angle of 90° was 7.9 kcps, slightly larger than that of water (4.1 kcps). The pH value of the as-obtained block copolymer at a concentration of 4.42 mg mL^{-1} of 6.0 reflects complete protonation of the NH_2 groups. When the block copolymer is added to the Eu-POM solution, the charge ratio γ_+ is defined as the fraction of the positive charge to total charges ($\gamma_+ = C_+/(C_+ + C_-)$, where C_+ and C_- denote the molar concentrations of the positive and negative charges, respectively). Changes in scattered intensity at three scattering angles and the hydrodynamic

[*] Prof. J. Zhang, Y. Liu, Y. Li, H. X. Zhao, Prof. X. H. Wan
Beijing National Laboratory for Molecular Sciences, Key Laboratory of Polymer Chemistry and Physics of Ministry of Education, College of Chemistry and Molecular Engineering, Peking University
Beijing 100871 (China)
E-mail: jz10@pku.edu.cn
xhwan@pku.edu.cn

[**] J.Z. and X.H.W. thank the Nation Science Foundation of China (No. 51003001; No. 20834001) for financial support. We appreciate Prof. Dehai Liang's supports with the laser light scattering instrument. Prof. Tianbo Liu and Panchao Yin at Lehigh University are greatly appreciated for helpful discussion.

Supporting information for this article is available on the WWW under http://dx.doi.org/10.1002/anie.201107481.

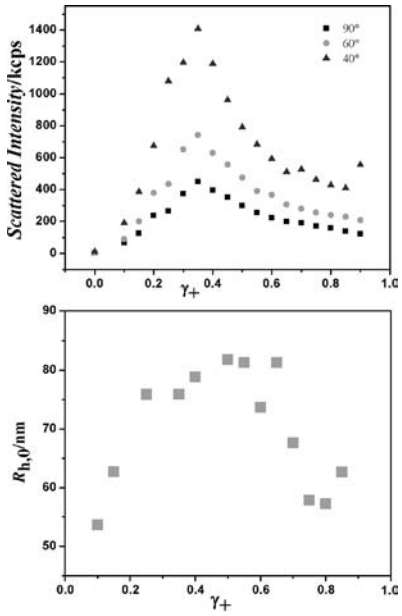

Figure 1. Plots of changes in excessive scattered intensity of POM solution during titration of block copolymer solution as a function of charge ratio γ_+ (top; kcps = kilocounts per second) and $R_{h,0}$ extrapolated from the R_h values at scattering angles of 90, 60, and 40° as a function of the charge ratio γ_+ (bottom).

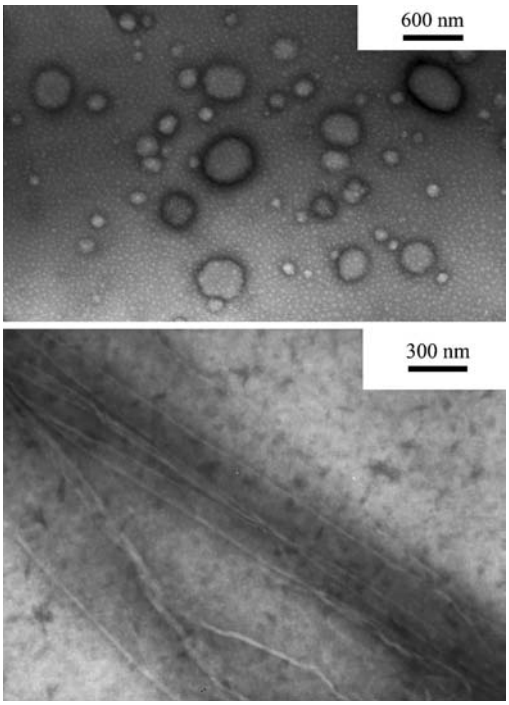

Figure 2. TEM images of POM–block copolymer complex at $\gamma_+ = 0.4$ (top) and $\gamma_+ = 0.85$ (bottom).

radius at zero angle ($R_{h,0}$) as a function of γ_+ during the titration are summarized in Figure 1. The ever-increasing scattered intensity indicates formation of the complex of Eu-POM with cationic PDMAEMA segments of the block copolymer. The scattered intensity reaches a maximum value of 448.9 kcps at $\gamma_+ = 0.35$. The R_h values of assemblies at different scattering angles are angle-dependent, and thus extrapolation was done to estimate $R_{h,0}$ at zero angle. During this stage, the average value of $R_{h,0}$ also increased from 54.5 ± 1.6 nm to 76.3 ± 2.3 nm. Afterwards, the intensity and R_h value decrease again. Interestingly, results from static light scattering show that the R_g value is very close to $R_{h,0}$ at various γ_+. For example, when $\gamma_+ = 0.5$, $R_g \approx 78.3 \pm 4$ nm is very close to $R_{h,0} \approx 81.8 \pm 2.4$ nm, which illustrates that a hollow structure of the C3M was formed. The $R_{h,0}$ value clearly decreased, to 56.5 ± 1.7 nm at $\gamma_+ \approx 0.8$, as did the intensity. It is known that the extent of complexation of C3M is highly dependent on the charge ratio of oppositely charged species, and it generally reaches a maximum at a stoichiometric condition of $\gamma_+ \approx 0.5$.[7,11] In the present work, a bias of $\gamma_+ \approx 0.35$ against isoelectric conditions reflects that the hollow assemblies are negatively overcharged. Noteworthily, the distribution of $R_{h,90}$ also become broader, owing to the contribution of large particles with $R_{h,90}$ greater than 1 μm.(see Supporting Information Figure S1) After γ_+ reaches 0.85, the intensity at three scattering angles and $R_{h,0}$ tend to increase again, but we could not obtain more reasonable information for $\gamma_+ > 0.85$, because large aggregates other than vesicles appeared and are not stable and strongly tend to precipitate during the short time period of the experiment.

Further proof for the formation of large assemblies during the whole titration process was obtained by TEM (Figure 2). For samples with $\gamma_+ \approx 0.3$–0.7, vesicles with an average diameter of about 200 nm were observed, which is in good agreement with the hollow structure revealed by the light-scattering experiments. When γ_+ is above 0.85, large aggregates, namely, nanobelts with an average diameter of 100 nm and length of several micrometers, were observed. Such large nanobelts have a strong tendency to precipitate from aqueous solution, and thus were practically beyond observation by light scattering.

The emission spectra of C3M in aqueous solutions at various γ_+ are shown in Figure 3. The absorption bands of POM complexes are similar to those of the pure POM and only became slightly stronger (Supporting Information Figure S3). All excitation wavelengths were 280 nm, corresponding to intramolecular energy transfer from the ligand-to-metal charge transfer (LMCT) band of O→W to the photoluminescent Eu^{3+} core.[12–14] The emission spectrum of discrete Eu-POM in aqueous solution displays all characteristic transitions of Eu^{3+} ($^5D_0 \rightarrow {}^7F_j$, $j = 0,1,2,3,4$), as indicated in Figure 3. As the block copolymer was added to the POM solution, the emission intensity increased dramatically, whereas the emission bands remained constant. At $\gamma_+ \approx 0.6$, the intensity of $^5D_0 \rightarrow {}^7F_2$ transition band $I_{(5D0 \rightarrow 7F2)}$ is about 21 times that of the discrete Eu-POM solution. The quantum yields of all complex solutions, determined by the relative method also increase about 20-fold, from 0.0051 to 0.1098. (Table 1) The emission of Eu^{3+} is highly dependent on its coordinated water, due to radiationless deactivation of the $^5D_0$ excited state through weak coupling with the vibrational states of high-frequency OH oscillators of water ligands.[12] Therefore, the remarkably enhanced emission of Eu^{3+} illustrates that Eu-POM is located in a relatively hydrophobic environment where the cationic

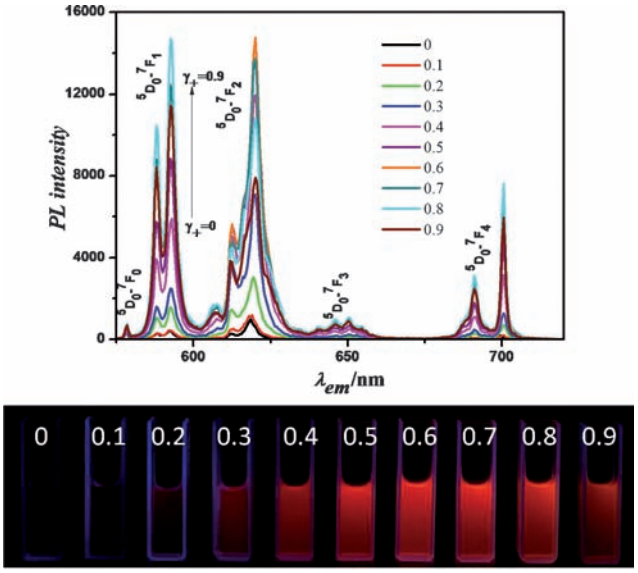

Figure 3. Emission spectra of Eu-POM and the block copolymer complex as a function of the positive charge ratio γ_+ at an excitation wavelength of 280 nm. The photograph of a series of complex solutions at the bottom was taken at an excitation wavelength of 254 nm.

Table 1: Summary of $I_{(5D0\text{-}7F2)}/I_{(5D0\text{-}7F1)}$, lifetimes τ_1 and τ_2, fractions of fluorophores α_1 and α_2, and quantum yield η, at various charge ratios γ_+.

Sample	γ_+	$I_{(D0\rightarrow F2)}/I_{(D0\rightarrow F1)}$	τ_1 [ms]	τ_2 [ms]	α_1	α_2	η
Eu-POM	–	2.179	0.240	–	1	0	0.0051
C3M	0.1	2.982	0.243	1.639	0.989	0.011	0.0126
C3M	0.2	2.576	0.267	1.806	0.942	0.058	0.0418
C3M	0.3	3.519	0.451	2.269	0.747	0.253	0.0521
C3M	0.4	2.598	0.675	3.018	0.710	0.290	0.0883
C3M	0.5	2.170	0.768	3.200	0.625	0.375	0.0948
C3M	0.6	1.638	0.897	3.213	0.478	0.522	0.1098
C3M	0.7	1.554	1.169	3.140	0.345	0.655	0.1165
C3M	0.8	1.180	1.391	3.162	0.293	0.707	0.0988
C3M	0.9	1.154	–	2.649	–	1	0.1064

PDMAEMA segments of the block copolymer have strong enough affinity to the anionic Eu-POM to replace water ligands through electrostatic interaction. Additionally, the hydrophobicity of the exterior PDMAEMA main chain may further prevent water molecules rebinding to Eu-POM.

The ratio of the integral intensity of $^5D_0\rightarrow{}^7F_2$ to $^5D_0\rightarrow{}^7F_1$ ($I_{(5D0\rightarrow7F2)}/I_{(5D0\rightarrow7F1)}$) is often used to evaluate the degree of variation of Eu^{3+} symmetry in different environments. As shown in Table 1, in the initial stage before $\gamma_+\approx0.3$, $I_{(5D0\rightarrow7F2)}/I_{(5D0\rightarrow7F1)}$ increased from 2.179 to 3.519, indicative of decreased symmetry of the microenvironment around Eu^{3+}.[15] It is known that the $EuW_{10}O_{36}^{9-}$ anion in initial aqueous solution coordinates with four water molecules and has C_{4v} symmetry.[13] As the block copolymer chains complex with the $EuW_{10}O_{36}^{9-}$ anion, the water molecules may be released and lead to a lower symmetry of Eu species. Afterwards, a decrease of $I_{(5D0\rightarrow7F2)}/I_{(5D0\rightarrow7F1)}$ beyond $\gamma_+\approx0.4$ reflects increased symmetry of the microenvironment around Eu^{3+}, which could be attributed to the fact that PDMEAMA segments have completely replaced water and Eu-POM molecules are located in the relatively homogenously distributed polymer matrix in the core.

The above hypothesis was further confirmed by the time-resolved emission. The lifetimes are summarized in Table 1. There was only one lifetime of about 0.240 ms for Eu-POM at a concentration of 0.1 mg mL^{-1}.[13] As long as the nonemissive block copolymer was added to the solution, double-exponential decays were present in all complex solutions (see Supporting Information Figure S2). At $\gamma_+=0.1$, besides the first lifetime τ_1 of discrete Eu-POM, a second lifetime $\tau_2\approx1.639$ ms appeared, which may be attributed to the complex of Eu-POM and block copolymer. The double-exponential intensity decay $I(t)$ can be expressed by Equation (1)

$$I(t)=I_1e^{-t/\tau_1}+I_2e^{-t/\tau_2} \quad (1)$$

$$\alpha_i=\frac{I_i}{I_1+I_2} \quad (2)$$

where the pre-exponential factors α_i ($i=1, 2$) represent the fraction of the fluorophore in each environment for the same fluorophore in different environments.[16] As shown in Table 1, τ_1 increases from 0.240 to 1.391 ms with γ_+ during the whole titration process, whereas τ_2 also increases with γ_+ until γ_+ reaches 0.4 and then remains almost constant at about 3.1 ms. The comparable value of τ_2 to that of Eu-POM in the solid state (2.9 ms)[17] suggests that it may be attributable to Eu-POM located in the very dense core of assemblies. The quantity τ_1 may be attributed to the single Eu-POM molecules and the increased decay time is due to replacement of the water ligands of Eu^{3+} by the block copolymer.

On the basis of the results of the fluorescence experiments and light scattering, a tentative mechanism of assembly during the titration process is proposed (Scheme 2). In the initial stage, Eu-POM associates with the PDMAEMA blocks through electrostatic attraction to form a loose intermediate structure (the nucleus); an equilibrium exists between the discrete Eu-POM and the nucleus. Afterwards the nuclei grow larger as more block copolymers are involved with increasing γ_+ value, accompanied by consumption of the single Eu-POM molecules. When the concentration of nuclei

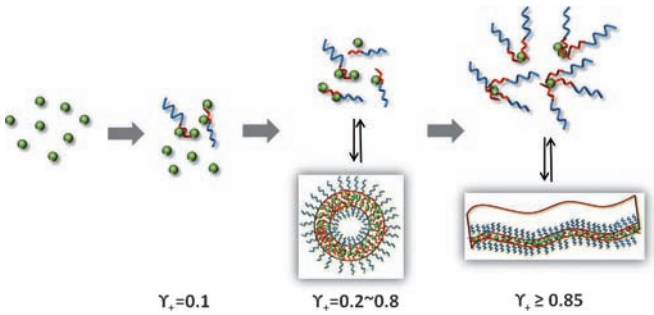

Scheme 2. Proposed tentative mechanism of self-assembly. The green particles stand for Eu-POM; the blue and red lines represent PEO and PDMEAMA blocks, respectively.

exceeds a certain value, they tend to assemble into bilayer vesicles with a relatively dense interior core of PMDEAMA-POM complexes and an exterior shell of PEO blocks. While the amount and size of vesicles changes in the assembly stage of $\gamma_+ = 0.2$–0.8, two Eu-containing species—one in the dense vesicles and the other in the loose nuclei—coexist in the solution. Finally, the nucleus has a structure in which one Eu-POM molecule is surrounded by a few block copolymer chains, and the dense nanostructures gradually evolve into nanosheets. The transition from vesicles to nanosheets may be due to a decrease in the interfacial energy of the nanostructure, that is, the core of Eu-POM-PDMAEMA became less hydrophobic while the content of hydrophilic PEO increased. Such a subtle balance of hydrophilic shell and hydrophobic core leads to formation of nanosheets.

The complexes are sensitive to ionic strength, as shown in Figure 4. With increasing addition of NaCl to the solution, the light scattering intensity continually decreased, as did R_h.

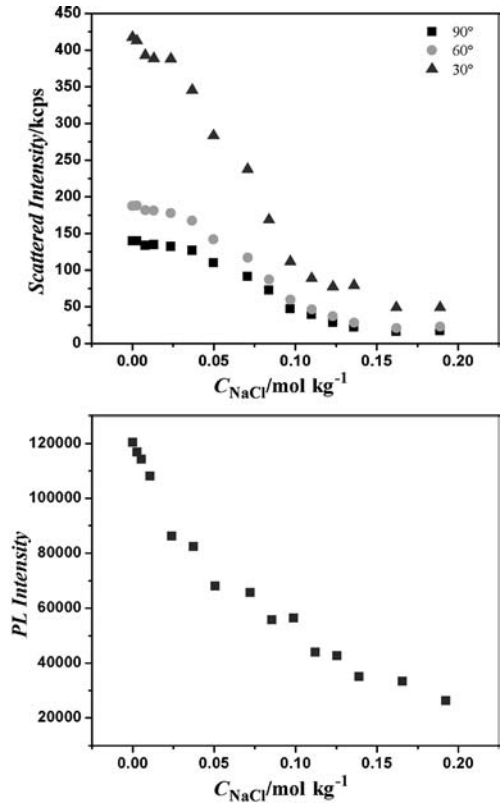

Figure 4. Changes of the scattered intensity and fluorescent intensity as a function of NaCl concentration.

Meanwhile, the emission intensity became weaker and the two lifetimes became shorter. The above results show that an increase in ionic strengths induces dissociation of the assemblies. The added small ions would bind individually to POM or PDMAEMA species, and weaken the electrostatic attraction between POM and PDMAEMA.

In summary, facile fabrication of core–shell nanostructures of a photoluminescent Eu-containing POM with double-hydrophilic neutral–cationic block copolymer PEO_{114}-*b*-$PDMAEMA_{16}$ in aqueous solution has been achieved through electrostatic interaction. The emission of Eu-POM was enhanced as much as 20 times through complexation with the cationic block PDMAEMA. The procedure is environmentally friendly, and biocompatibility is enhanced due to the absence of trace impurities from preparation protocols involving organic solvents. Such a self-assembly route endows the Eu-POM fluorescent materials with potential biomedical applications as stimuli-responsive carriers for bioimaging and biodetection. Applying this simple assembly method to other POMs would expand their field of application. Future work will focus on exploring POM hybrids with catalytic, magnetic, and electrooptical functionality.

Experimental Section

$Na_9EuW_{10}O_{36}{\cdot}32\,H_2O$ was prepared as describe by Yamase.[12] An appropriate amount of $Na_9EuW_{10}O_{36}{\cdot}32\,H_2O$ was dissolved in water to make a solution with a concentration of 0.1 mg mL^{-1}. Block copolymer PEO_{114}-*b*-$PDMAEMA_{16}$ (PDI = 1.2) was purchased from Polymer Source, Canada, and used as obtained. PEO_{114}-*b*-$PDMAEMA_{16}$ in aqueous solution was added dropwise to the $Na_9EuW_{10}O_{36}$ solution to prepare complex solutions with various charge ratios. For laser light scattering measurements, the polymer solution and the POM solution were separately filtered directly into dust-free light-scattering cells through filters with 0.2 μm pore size. Afterwards, the block polymer solution was added dropwise to the POM solution by using a Hamilton microsyringe, and each increment of the charge ratio γ was about 0.05. After addition of the block copolymer solution, the POM solutions were slightly shaken and allowed to sit at 25 °C for at least 20 min to reach equilibrium, which was evaluated by the time dependence of the scattered intensity. The whole titration process was monitored by laser light scattering. A commercial laser light scattering spectrometer (Brookhaven Inc, Holtsville, NY) equipped with a BI-200SM goniometer and a BI-TurboCorr digital correlator was used to perform both static light scattering (SLS) and dynamic light scattering (DLS) over a scattering angle range of 20 to 150°. A 100 mW vertically polarized solid-state laser (GNI, Changchun, China) operating at 532 nm was used as light source. The intensity–intensity time-correlation function was analyzed by the COTIN method. In SLS, The excess scattered intensities of the complex solution were collected by deduction of scattered intensities of the block copolymer. The angular dependence of the excess absolute time-averaged scattering intensity was measured. The principle of laser light scattering was presented in previous publications.[18]

Photoluminescence measurements were performed on an FLS 920 Steady State & Time-resolved Fluorescence Spectrometer (Edinburgh Instruments Ltd.). The complex solutions were prepared by the same titration procedure as for the light scattering experiments. The quantum yields of the complex solution were determined by the relative method with tryptophan as standard, excited at 280 nm.

TEM images were obtained on a JEM-100CXTEM instrument operating at an acceleration voltage of 100 kV. A drop of sample solution was mixed with a drop of 2% (w/v) aqueous solution of uranyl acetate. The mixture was deposited onto a carbon-coated copper EM grid for a few minutes. Excess solution was blotted away with a strip of filter paper, and the sample grid was dried in air.

Received: October 24, 2011
Revised: December 5, 2011
Published online: March 27, 2012

Keywords: block copolymers · lanthanides · luminescence · polyoxometalates · self-assembly

[1] C. L. Hill, *Chem. Rev.* **1998**, *98*, 1. And the entire issue.
[2] a) A. Müller, S. Roy, *Coord. Chem. Rev.* **2003**, *245*, 153 – 166; b) A. Dolbecq, E. Dumas, C. R. Mayer, P. Mialane, *Chem. Rev.* **2010**, *110*, 6009 – 6048.
[3] a) K. Binnemans, *Chem. Rev.* **2009**, *109*, 4283 – 4374; b) T. Yamase, *Chem. Rev.* **1998**, *98*, 307 – 325.
[4] W. Qi, L. X. Wu, *Polym. Int.* **2009**, *58*, 1217 – 1225.
[5] a) H. L. Li, W, Qi, W. Li, H. Sun, W. F. Bu, L. X. Wu, *Adv. Mater.* **2005**, *17*, 2688 – 2692; b) W. F. Bu, S. Uchida, N. Mizuno, *Angew. Chem.* **2009**, *121*, 8431 – 8434; *Angew. Chem. Int. Ed.* **2009**, *48*, 8281 – 8284.
[6] a) Y. K. Han, X. Yu, Z. J. Zhang, B. Liu, P. Zheng, S. J. He, W. Wang, *Macromolecules* **2009**, *42*, 6543 – 6548; b) Y. K. Han, Z. J. Zhang, Y. L. Wang, N. Xia, B. Liu, Y. Xiao, L. X. Jin, P. Zheng, W. Wang, *Macromol. Chem. Phys.* **2011**, *212*, 81 – 87.
[7] I. K. Voets, A. de Keizer, M. A. Cohen Stuart, *Adv. Colloid Interface Sci.* **2009**, *147 – 148*, 300 – 318, and references therein.
[8] A. Harada, K. Kataoka, *Prog. Polym. Sci.* **2006**, *31*, 949 – 982.
[9] Y. Lee, S. Fukushima, Y. Bae, S. Hiki, T. Ishii, K. Kataoka, *J. Am. Chem. Soc.* **2007**, *129*, 5362 – 5363.
[10] a) B. Liu, G. C. Bazan, *Chem. Mater.* **2004**, *16*, 4467 – 4476; b) B. Liu, G. C. Bazan, *J. Am. Chem. Soc.* **2004**, *126*, 1942 – 1943.
[11] J. F. Berret, *Macromolecules* **2007**, *40*, 4260 – 4266.
[12] M. Sugeta, T. Yamase, *Bull. Chem. Soc. Jpn.* **1993**, *66*, 444 – 447.
[13] R. Ballardini, Q. G. Mulazzani, M. Venturi, F. Bolletta, V. Balzani, *Inorg. Chem.* **1984**, *23*, 300 – 305.
[14] T. Yamase, M. Sugeta, *J. Chem. Soc. Dalton Trans.* **1993**, 759 – 765.
[15] a) M. Nogami, Y. Abe, *J. Non-Cryst. Solids* **1996**, *197*, 73 – 78; b) J. A. Capobianco, P. P. Proulx, M. Bettinelli, F. Negrisolo, *Phys. Rev. B* **1990**, *42*, 5936 – 5944.
[16] J. R. Lakowicz, *Principles of Fluorescence Spectroscopy*, 3rd ed., Springer, Berlin, **2006**, pp. 101 – 103.
[17] a) W. Bu, H. Li, W. Li, L. X. Wu, C. Zhai, Y. Wu, *J. Phys. Chem. B* **2004**, *108*, 12776 – 12782; b) T. R. Zhang, C. Spitz, M. Antonietti, C. F. J. Faul, *Chem. Eur. J.* **2005**, *11*, 1001 – 1009.
[18] a) J. Zhang, D. Li, G. Liu, K. J. Glover, T. B. Liu, *J. Am. Chem. Soc.* **2009**, *131*, 15152 – 15159; b) J. Zhang, Y. F. Song, L. Cronin, T. B. Liu, *J. Am. Chem. Soc.* **2008**, *130*, 14408 – 14409.